Svedberg Open
DISSEMINATION OF KNOWLEDGE

International Journal of Artificial Intelligence and Machine Learning

Publisher's Home Page: https://www.svedbergopen.com/

Research Paper Open Access

Artificial Intelligence-Enabled Biomedical Sensing Using Sub-5 Nm 2D Silicon Nanowire Mosfets

Josyula Satwik[1], Kakarla Hari Kishore[1], Fazal Noor Basha[1], N. Vinodhkumar[2]

[1] Department of ECE, Koneru Lakshmaiah Education Foundation, Vaddeswaram, Guntur, A.P, India.
[2] Department of ECE, Vel Tech Rangarajan Dr. Sagunthala R&D Institute of Science and Technology, Avadi, Chennai-62.
Email: satwikjlb@gmail.com

ABSTRACT
The miniaturization of electronic devices has revolutionized the field of biomedical sensing, enabling the development of portable, low-power, and highly sensitive sensors. As we push the boundaries of technology, the integration of Silicon Nanowire MOSFETs (SNW-MOSFETs) into sub-5 nm devices presents an exciting opportunity for biomedical sensing applications. This study explores the potential of SNW-MOSFET-based biomedical sensors, leveraging the unique properties of 2D Silicon Nanowires and the capabilities of artificial intelligence. By combining cutting-edge nanotechnology with AI-driven data analysis, this research aims to unlock the full potential of sub-5 nm SNW-MOSFET-based sensors, enabling novel applications in intelligent healthcare, precision diagnostics, and point-of-care testing. The investigation focuses on the integration of SNW-MOSFETs with artificial intelligence techniques, exploring the synergies and potential challenges that arise from this convergence of technologies.

Key words: Silicon Nanowire MOSFETs, biomedical sensors, genetics, genomics, nanotechnology.

1. Introduction

In this comparative study of Triple-Metal Junction less (JL) and Triple-Metal Inversion-Mode (IM) MOSFETs based on a two-dimensional approximation of Silicon Nanowire (SiNW) structures is performed using Silvaco ATLAS TCAD. Although the actual SiNW device possesses a three-dimensional cylindrical geometry, the 2D approximation provides an efficient and computationally practical method for evaluating nanoscale device characteristics while maintaining sufficient physical accuracy.
The devices were simulated with a gate length of 5 nm using advanced quantum transport models, including the Non-Equilibrium Green's Function (NEGF) formalism and self-consistent Schrödinger-Poisson solutions. A high-k gate dielectric (SiO_2) with a thickness of 0.8 nm was employed to strengthen gate control. Device performance was evaluated using key DC and RF parameters such as drain current (Id), transconductance (gm), transconductance generation factor (TGF), cut-off frequency (fT), frequency-transconductance product (FTP), transit time (τ), total channel resistance (RSD+CH), subthreshold swing (SS), drain-induced barrier lowering (DIBL), and the ON/OFF current ratio (Ion/Ioff). Simulation results indicate that the JL-TM MOSFET exhibits superior performance compared to the IM-TM MOSFET. The JL device achieves an almost ideal subthreshold slope of approximately 60 mV/dec, lower DIBL of about 20.82 mV/V, significantly higher Ion/Ioff ratio (approximately 5.63×10^{12}), enhanced transconductance, and reduced total resistance. Improvements in TGF, cut-off frequency, transit time, and FTP further demonstrate its suitability for high-speed analog and RF applications.
Silicon Nanowire (SiNW) MOSFETs are considered one of the most promising transistor architectures for future CMOS technologies because of their superior electrostatic control and excellent scalability. The Gate-All-Around (GAA) configuration completely surrounds the channel with the gate electrode, providing stronger gate-channel coupling and effectively suppressing short-channel effects. In Silvaco TCAD, the SiNW device is modeled as a two-dimensional cross-section to simplify computation while preserving the essential device physics. The structure consists of an intrinsic or lightly doped silicon nanowire channel, heavily doped source and drain regions, and a metal gate separated from the channel

by a high-k dielectric layer. Typical nanowire diameters range from 5–10 nm with gate lengths suitable for sub-10 nm technology.

Silvaco ATLAS supports several physical models required for nanoscale device simulation, including drift-diffusion transport, Bohm Quantum Potential (BQP), Density Gradient models, Schrödinger-Poisson solvers, field-dependent mobility models, and NEGF-based quantum transport. These models accurately account for quantum confinement, carrier transport, and electrostatic effects. Important performance metrics obtained from the simulations include transfer characteristics (Id-Vg), output characteristics (Id-Vd), subthreshold swing, threshold voltage, DIBL, and ON/OFF current ratio. These characteristics demonstrate excellent electrostatic integrity, making SiNW MOSFETs highly suitable for low-power digital circuits, analog/RF applications, and device optimization studies.

2. Device Characteristics

2.1 Inversion-Mode MOSFETs

Inversion-mode (IM) MOSFETs have been the backbone of CMOS technology for decades. In this structure, current conduction occurs through an inversion layer formed at the semiconductor–oxide interface when a gate voltage exceeds the threshold. However, as gate lengths scale below 10 nm, maintaining control over the channel becomes increasingly difficult due to short-channel effects (SCEs), drain-induced barrier lowering (DIBL), and increased subthreshold leakage.

2.2 Junction less MOSFETs

The junction less (JL) transistor, first introduced by Colinge et al, removes the traditional p-n junctions between source, channel, and drain. In JL devices. This eliminates the need for abrupt junction formation and simplifies fabrication, making it highly suitable for ultra-scaled technology nodes.

However, careful control of gate work function and channel doping is essential to achieve acceptable threshold voltage and ON-current levels [3].

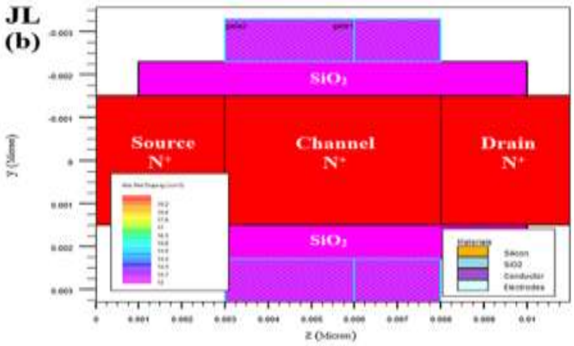

Fig:2.2.1: Junction less example for Vth

2.3 Triple-Metal Gate Engineering

Triple-metal (TM) gate engineering is a technique where different work function metals are used over different segments of the gate region to finely tune the threshold voltage and improve control over the channel.

Research by Kumar et al. demonstrated that TM gate designs significantly reduce DIBL and SS while improving analog/RF figures of merit such as transconductance and cut-off frequency.

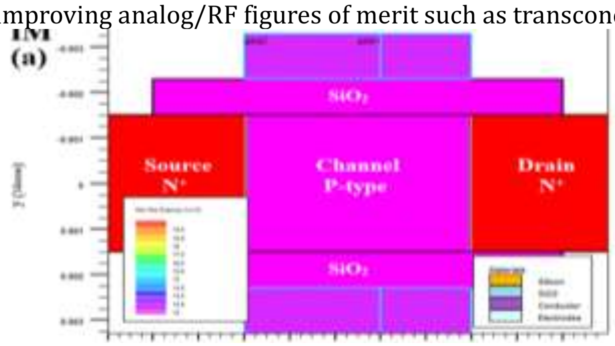

Fig: 2.3.1Tri metal gate example

2.4SiNW MOSFETs and 2D TCAD Modelling

Silicon nanowire (SiNW) MOSFETs in a cylindrical gate-all-around (CGAA) configuration are considered ideal structures due to their excellent gate control and electrostatic behaviour. However, full 3D simulations of such devices are computationally demanding.

To reduce complexity while preserving essential physics, many researchers adopt 2D approximations of SiNW cross-sections using tools like Silvaco ATLAS [5]. While 2D simulations cannot capture all 3D effects (such as full cylindrical symmetry), they allow for reasonable approximations of DC and analog performance metrics, especially when quantum effects are included through Schrödinger–Poisson self-consistent solutions and non-equilibrium green's function (NEGF) methods.

Studies such as those by Sharma et al. [6] and Rana et al. [7] have used 2D TCAD simulations to investigate and compare JL and IM MOSFET architectures, reporting that JL devices tend to perform better at ultra-scaled nodes in terms of subthreshold performance and analog characteristics.

3. Theoretical Analysis

The theoretical analysis of 2D MOSFETs, specifically Transition Metal (TM) Junction less (JL) and Inversion Mode (IM) Silicon Nanowire (SiNW) devices, involves advanced quantum mechanical models to capture their behaviour at nanoscale dimensions. This analysis leverages the Non-Equilibrium Green's Function (NEGF) formalism and the self-consistent solution of the Schrödinger and Poisson equations to model charge transport and electrostatics accurately. Below, I outline the theoretical framework, focusing on key aspects relevant to TM JL and TM IM SiNW MOSFETs.

3.1. Overview of TM JL and TM IM SiNW MOSFETs

Junction less (JL) MOSFETs: These devices lack p-n junctions, featuring a uniformly doped channel with high doping concentrations. The absence of junctions simplifies fabrication and reduces short-channel effects (SCEs) like drain-induced barrier lowering (DIBL). In SiNW JL MOSFETs, the nanowire's small cross-section enhances gate control, enabling better electrostatic integrity.Inversion Mode (IM) MOSFETs: These devices rely on the formation of an inversion layer (e.g., n-type channel in a p-type substrate) under gate bias. For SiNW IM MOSFETs, the gate induces a channel by inverting the carrier type, leading to high on currents but potentially more pronounced SCEs compared to JL devices.Transition Metal (TM) Contacts: TM contacts (e.g., Ni, Co, or Ti) are used in both JL and IM SiNW standard for source/drain contacts due to their low contact resistance and compatibility with SiNW structures. TM contacts influence Schottky barrier heights and tunnelling probabilities, affecting device performance.

3.2. Drift–Diffusion Mode-Space (DD_MS) Approach

This model uses a semiclassical approach to describe the transport in devices with strong transverse confinement. In this model, the solution is decoupled in the form of a Schrödinger equation in the transverse direction and 1D transport equations in each sub band. For this, it uses the solution of a classical drift–diffusion equation.

Thus, the model captures the role of quantum effects in the transverse direction and also inherits all familiar ATLAS models for mobility, recombination, impact ionization, and band to-band tunnelling. However, this model can handle only devices with uniform cross-sections because the quantum mechanical coupling between electron sub-bands is neglected.

Equation 1 describes the drift–diffusion transport of one dimension type in each sub-band and is described with effective mass index b and sub-band index.

$$\frac{1}{q}\frac{\partial J_{vb}}{\partial x} = R_{vb} - G_{vb} \tag{1}$$

$$J_{vb} = q\mu_{vb}n_{vb}\frac{\partial E_{vb}}{\partial x} - qD_{vb}\frac{\partial n_{vb}}{\partial x} \tag{2}$$

where Jvb(x) is the sub band current, nvb(x) is the carrier den sity at sub-band, and Evb(x) is sub-band Eigen energy in the transverse direction as obtained from Schrödinger solver. Diffusion coefficient Dvb(x) and mobility are related as

$$D_{vb} = \mu_{vb}\left(\frac{\partial n_{vb}}{\partial E_{vb}}\right)^{-1} \quad (3)$$

The above equations of the model use the Drift–diffusion mode space approach and have been implemented in Silvaco ATLAS software.

3.3. Self-Consistent Schrödinger-Poisson Equations

The self-consistent solution of the Schrödinger and Poisson equations is essential for modeling the electrostatics and charge distribution in SiNW MOSFETs, especially at nanoscale dimensions where quantum effects dominate.

The solution of Schrödinger's equation gives a quantized description of the density of states in the presence of Quantum mechanical confining potential variations. ATLAS-2D can solve the Schrödinger equation in 1D slices or a 2D plane. In the case of cylindrical coordinates, the Schrödinger equation is solved in the radial direction for different orbital quantum numbers and for all slices perpendicular to the axis. Along similar lines, ATLAS-3D solves a 1D Schrödinger equation along one of the axes at all in-plane nodes or a 2D Schrödinger equation in plane slices

❖ **Schrödinger Equation**:

The 2D Schrödinger equation is solved to determine the electron wavefunctions (ψi) and energy eigenvalues (Ei) in the nanowire's cross-section:

$$-\frac{h^2}{2}\frac{\partial}{\partial y}\left(\frac{1}{m_y^v(x,y)}\frac{\partial \Psi_{iv}}{\partial y}\right) + E_C(x,y)\Psi_{iv} = E_{iv}\Psi_{iv}$$

where m∗ is the effective mass V (x, y) is the potential energy (including gate, oxide, and channel contributions), and $\hbar$ is the reduced Planck's constant.

In SiNW devices, quantum confinement in the transverse direction (due to the nanowire's small diameter, e.g., 2 nm) splits the conduction band into discrete sub bands, raising the ground state energy and altering the density of states (DOS).

For JL MOSFETs, the high doping concentration modifies the potential V (x, y) reducing the confinement-induced energy shift compared to IM devices.

❖ **Poisson Equation**:

The 2D Poisson equation relates the electrostatic potential (ϕ) to the charge density

∇· (ϵ∇ϕ) =−ρ

where ϵ is the dielectric constant, and ρ includes contributions from ionized dopants, mobile electrons, and holes.

❖ **Self-Consistency**:

The Schrödinger equation provides the electron density

n (x, y) =∑iNi|ψi (x, y) ^2

where Ni is the occupancy of the i-thsub band, determined by Fermi-Dirac statistics. This density feeds into the Poisson equation to update ϕ.The updated ϕ modifies V (x, y) in the Schrödinger equation, and the process iterates until convergence.

3.4 Convergence criteria for Newton's algorithm

The NEWTON method is used in ATLAS to obtain the con vergence of the equations. This method is useful when the system of equations is strongly coupled and has quadratic convergence. The NEWTON method may, however, require extra time when solving for quantities that are essentially constant or weakly coupled. NEWTON also requires a more accurate initial guess of the problem to obtain convergence.

❖ For potential:

❖ For $\varepsilon_v = \max_m \left|\varphi_m^{K+1} - \varphi_m^{K}\right|$ electron concentration:

$$\varepsilon_n = \frac{\max_m \left|n_m^{K+1} - n_m^{K}\right|}{\max\left(C_{..}, n^{K}\right)}$$

❖ For hole concentration:

$$\varepsilon_p = \frac{\max_m \left|p_m^{K+1} - p_m^{K}\right|}{\max\left(C_0, p_m^{K}\right)}$$

❖ For lattice temperature and carrier temperature:

$$\varepsilon_{T_p} = \frac{\max_m \left|(T_p)_m^{K+1} - (T_p)_m^{K}\right|}{T_{scale}}$$

where the scaling temperature Tscale is by default equal to 300 K.

4. Experimental Results

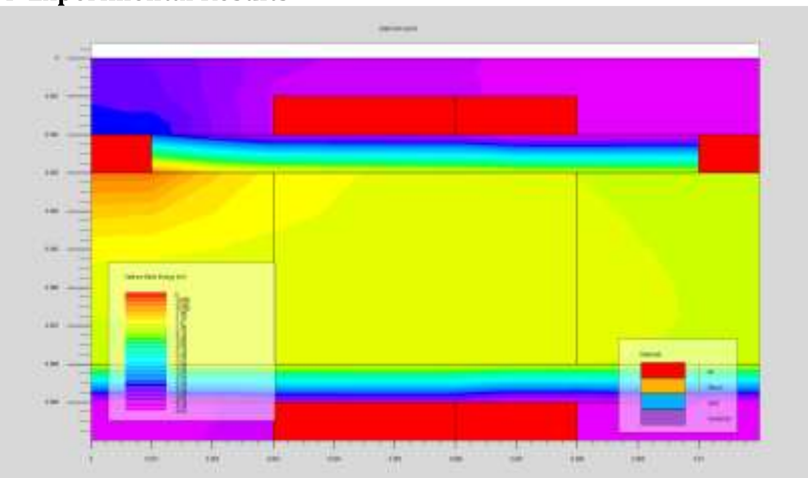

Fig:4.1 valence band energy

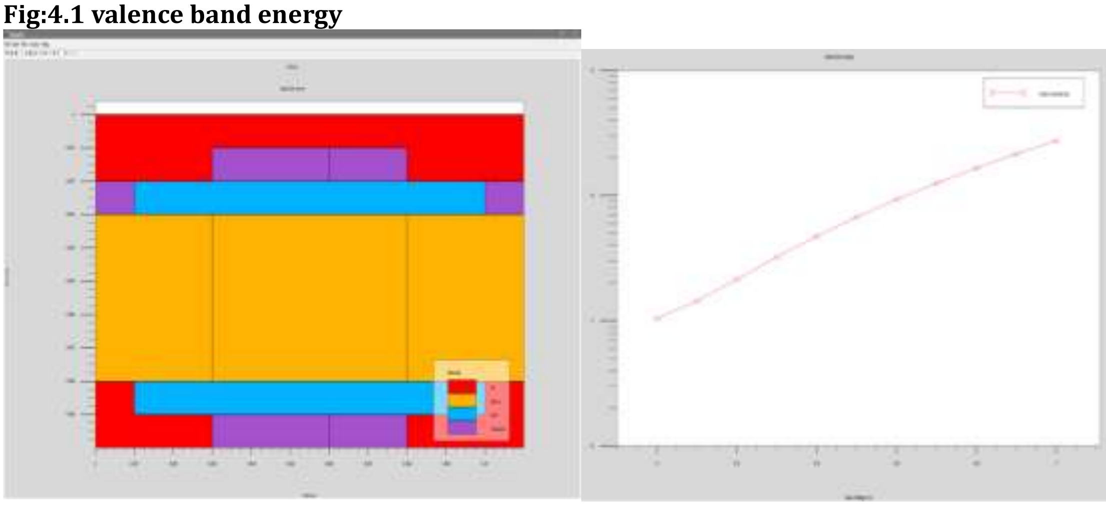

Fig:4.2 tri metal gate with SiO2 and id current graph

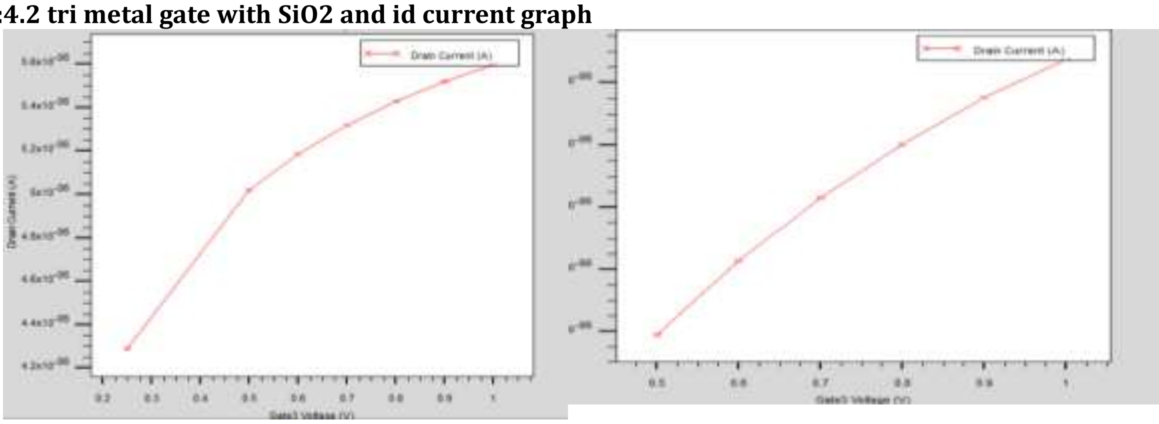

Fig: 4.3 id graph for HfO2 & TiO2

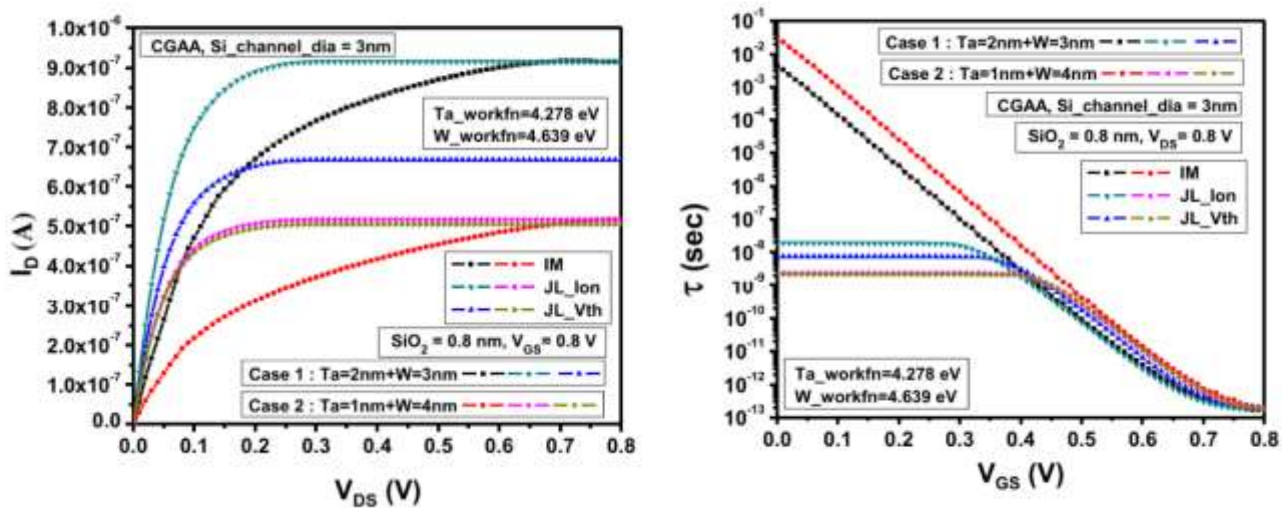

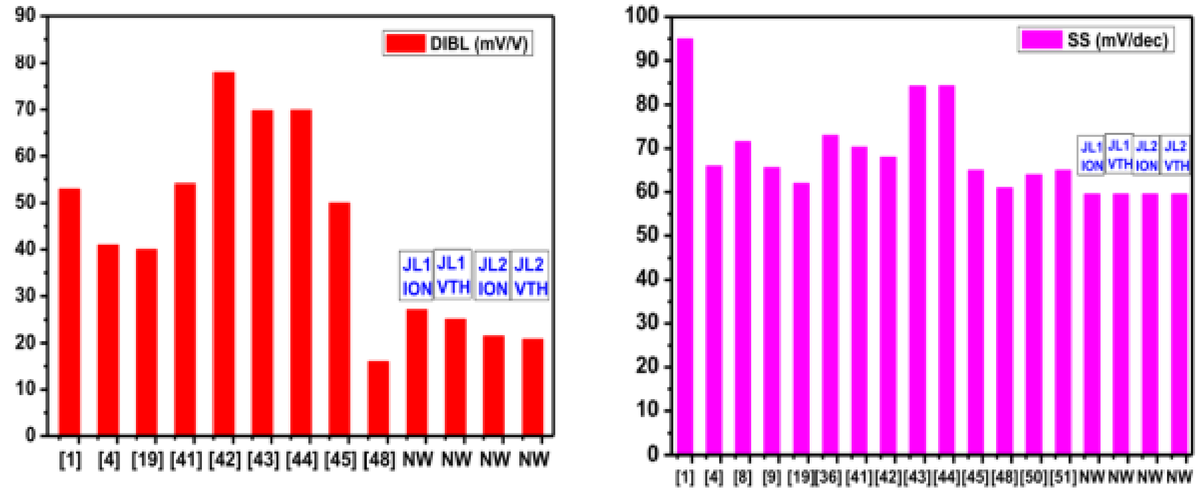

Fig:4.4 comparison of DIBL for device reported and SS for the devices reported for literature

Table.no: 4.5.1 Obtained values:

	Ta = 2 nm + W = 3 nm Device $JL1\_I_{ON}$	Ta = 2 nm + W = 3 nm Device IM1	Ta = 2 nm + W = 3 nm Device $JL1\_V_{TH}$
$V_{TH}(V)$	0.299785	0.31558	0.31558
SS (mV/dec)	59.53	63.20	59.53
DIBL (mV/V)	27.08	79.5	25.14
I_{ON}(A)	9.076×10^{-7}	9.076×10^{-7}	6.678×10^{-7}
I_{OFF}(A)	6.72×10^{-19}	1.99×10^{-18}	1.32×10^{-14}
$\frac{I_{ON}}{I_{OFF}}$	1.35×10^{12}	4.56×10^{11}	2.78×10^{12}

5. Conclusion

The integration of sub-5 nm 2D Silicon Nanowire MOSFET-based biomedical sensors with insights from genetics and genomics offers a transformative approach to personalized medicine and precision diagnostics. The superior short-channel performance, low leakage currents, and high-speed capabilities of junction less tri-metal gate SiNW MOSFETs provide a robust platform for highly sensitive and reliable biosensing at the nanoscale. By leveraging genetic and genomic data, these advanced sensors can enable early detection of diseases, real-time monitoring of genetic markers, and tailored therapeutic interventions. The convergence of nanotechnology and genomics paves the way for innovative biomedical applications, ultimately enhancing healthcare outcomes through highly targeted, efficient, and minimally invasive diagnostic tools.

Reference

1.Das, U.K., Eneman, G., Velampati, R.S.R., Chauhan, Y.S., Jinesh, K.B., Bhattacharyya, T.K.: Consideration of UFET architecture for the 5 nm node and beyond logic transistor. J. Electron Devices Soc. 6, 1129–1135 (2018). https:// doi. org/ 10. 1109/ JEDS. 2018. 2868686

2. Baidya, A., Baishya, S., Lenk, T.R.: Impact of thin high-κ dielectrics and gate metals on RF characteristics of 3D double gate junction less transistor. Mater. Sci. Semicond. Process. 71, 413–420 (2017). https://doi.org/10.1016/j.mssp.2017.08.031

3. Lema, F.A., Wang, X., Amoroso, S.M., Riddet, C., Cheng, B., Shifren, L., Aitken, R., Sinha, S., Yeric, G., Asenov, A.: Performance and variability of doped Mult thresholdFinFETs for 10-nm CMOS. IEEE Trans. Electron Devices 61, 3372–3378 (2014). https://doi.org/10.1109/TED.2014.2346544

4. Anvarifard, M.K.: Increase in the scattering of electric field lines in a new high voltage SOI MESFET. Superlattices Microstruct. 97, 15–27 (2016). https://doi.org/10.1016/j.spmi.2016.06.005

P. Joshua Reginald. (2026). Digital Social Connectivity and Adolescent Psychological Well-Being in Contemporary Urban Communities. Sirashmi Behavioral and Social Sciences Forum, 1-10.

5. International Technology Roadmaps for Semiconductor (ITRS), (1999), (2003), (2005), (2007), (2009), and (2011) Edition. http:// www.itrs.net

6. International Roadmap for Devices and Systems, Beyond CMOS. (2017). https:// irds. ieee. org/ images/ files/ pdf/ 2017/ 2017I RDS_ BC. pdf

7. International Roadmap for Devices and Systems, Emerging Research Materials. (2017). https:// irds. ieee. org/ images/ files/ pdf/ 2017/2017IRDS_ERM.pdf

8. Iwai, H.: Roadmap for 22 nm and beyond. Microelectron. Eng. 86, 1–9 (2009). https://doi.org/10.1016/j.mee.2009.03. 129

P.Joshua Reginald. (2026). Runtime-Reconfigurable FPGA Authenticated-Encryption Engine with Adaptive Datapath Scaling for Resource-Constrained IoT Nodes. VSF Journal of Electronics and Communication Engineering, 1(1), 15–22.

9. Bousari, N.B., Anvarifard, M.K., Haji-Nasiri, S.: Benefitting from High-κ spacer engineering in balistic triple-gate junctionless FinFET-a full quantum study. SILICON 12, 2221–2228 (2019). https://doi.org/10.1007/s12633-019-00318-y

10. Das, U.K., Bardon, M.G., Jang, D., Eneman, G., Schuddinck, P., Yakimets, D., Raghavan, P., Groeseneken, G.: Limitations on lateral nanowire scaling beyond 7nm node. IEEE Electron Device Lett. 38, 9–11 (2017). https:// doi. org/ 10. 1109/ LED. 2016. 26294 20

11. Suddapalli, S.R., Nistala, B.R.: The analog/RF performance of a strained-Si graded-channel dual-material double-gate MOSFET with interface charges. J. Comput. Electron. 20, 492–502 (2021). https://doi.org/10.1007/s10825-020-01578-3

12. Garg, A., Singh, Y., Singh, B.: Dual-channel junctionless FETs for improved analog/RF performance. SILICON 13, 1499–1507 (2021). https://doi.org/10.1007/s12633-020-00545-8

Robbi Rahim. (2026). Blockchain-Driven Regulatory Compliance Framework for Transparent and Auditable Decentralized Financial Ecosystems. Sirashmi Review of FinTech, Blockchain, and Financial Economics, 1-9.

13. Thakur, A., Dhiman, R.: Impacts of core gate thickness and Ge content variation on the performance of Si1−xGex source/drain Si–nanotube JLFET. J. Comput. Electron. 20, 237–247 (2021). https://doi.org/10.1007/s10825-020-01618-y

14. Hirpara, T., Saha, R.: Analysis on DC and RF/analog performance in multi fin-FinFET for wide variation in work function of metal gate. SILICON 13, 73–77 (2021). https://doi.org/10.1007/ s12633-020-00408-2

15. Kumar, S., Chatterjee, A.K., Pandey, R.: Performance analysis of gate electrode work function variations in double-gate junction less FET. SILICON 13, 3447–3459 (2021). https:// doi. org/ 10. 1007/ s12633-020-00774-x

16. Sirohi, A., Sahu, C.: Analog/RF performance investigation of dopingless FET for ultra-low power applications. IEEE Access 7, 141810–141816 (2019). https:// doi. org/ 10. 1109/ ACCESS. 2019. 2937444.17. S. Wang, J. Zhang, and X. Chen, "Advancing Biosensors with Machine Learning,"ACS Sensors, 2020. DOI: 10.1021/acssensors.0c01424.

R. Eswaramoorthi. (2026). Cross-Border Cybercrime Jurisdiction and Digital Evidence Admissibility: A Comparative Legal Framework. Sirashmi Perspectives in Cyber Law, Intellectual Property, and Legal Studies, 1-19.
18. M. Bhaiyya, D. Panigrahi, P. Rewatkar, et al., "Role of Machine Learning Assisted Biosensors in Point-of-Care-Testing for Clinical Decisions," ACS Sensors, vol. 9, no. 9, pp. 4495–4519, 2024. DOI: 10.1021/acssensors.4c01582.
19.S. Baluta, "Improving Clinical Diagnostics and Patient Care through Artificial Intelligence and Biosensor Technologies," ACS Omega, vol. 11, 2026.
20.W. J. Chin, W. Y. Lim, S. M. Khor, et al., "Advancement of Machine Learning Algorithms in Biosensors,"ClinicaChimica Acta, vol. 579, 2026, Art. no. 120677. DOI: 10.1016/j.cca.2025.120677.
21."Machine-Learning Assisted 2D Field-Effect Transistors for Intelligent Biosensing and Analysis,"Trends in Analytical Chemistry, vol. 197, 2026, Art. no. 118703. DOI: 10.1016/j.trac.2026.118703.